

# Improved ab Initio Calculations of Amplitude and Phase Functions for Extended X-ray Absorption Fine Structure Spectroscopy<sup>†</sup>

A. G. McKale,<sup>\*,‡,§,⊥</sup> B. W. Veal,<sup>⊥</sup> A. P. Paulikas,<sup>⊥</sup> S.-K. Chan,<sup>⊥</sup> and G. S. Knapp<sup>||</sup>

Contribution from the Argonne National Laboratory, Argonne, Illinois 60439, and Surface Science Instruments, Mountain View, California 94043. Received July 20, 1987

**Abstract:** Extended X-ray absorption fine structure (EXAFS) backscattering amplitude and phase functions have been calculated from first principles for K and L edges for nearly every element in the periodic table by using a full curved wave formalism. These functions are tabulated for approximately half of the elements from boron through californium. The functions are calculated for the range  $2 \leq k \leq 20 \text{ \AA}^{-1}$ , thus extending the range of currently available calculations to both higher and lower  $k$ . The range of elements has also been extended to include the actinide series. Because a curved wave formalism has been used for these calculations, the functions for  $L_{III}$  absorption edges are different from those of K (or more generally, s-shell) absorption edges. Variations of the functions for K and  $L_{III}$  absorption are illustrated. These ab initio calculations can be used in EXAFS data analysis to provide structural (interatomic distances) and chemical (type of neighboring atoms, Debye Waller factor) information with improved accuracy.

Extended X-ray absorption fine structure (EXAFS) is the oscillatory modulation of the X-ray absorption coefficient as a function of energy above an X-ray absorption edge. During the 1970s it was recognized that these spectra contain local structural information, and methods for extracting it were developed. The subsequent availability of synchrotron radiation greatly improved the speed of data acquisition and the quality of data that could be obtained. These developments established EXAFS as a practical and widely used structural tool.<sup>1</sup>

The structural parameters that can be obtained from EXAFS include the number of neighbors surrounding the absorber, their distances from it, and their MSR (mean-square relative displacement from the absorbing atom). In order to extract information about the local environment of the absorber, however, the backscattering amplitude  $B(k)$  and phase shift functions  $\Phi(k)$  are needed. The term  $\Phi(k)$  is a sum of contributions,  $\delta_c(k)$ , from the absorber, and  $\phi(k)$  from the scattering atom. These functions can be obtained experimentally from EXAFS spectra of model compounds.<sup>1</sup> However, obtaining an appropriate model compound and extracting the amplitude and phase functions may be difficult.

In the late 1970s, Teo and Lee<sup>2</sup> published a tabulation of theoretically determined amplitude and phase shift functions. It was their hope that such a tabulation would eliminate the need for measurement of model compounds, resulting in a major savings in time and effort, and would eliminate errors that might come from measurement and analysis of model compounds. Their calculations have proven to be extremely valuable for analysis of EXAFS spectra. Their work also supplies insight into the systematic variation of these functions with  $Z$  that would be otherwise very difficult to obtain. For high accuracy analysis, however, especially for the heavier elements, it still remains necessary to extract the functions from measurements of model compounds.

Recent studies have indicated that the single scattering EXAFS theory is valid to much lower energies than previously believed.<sup>3,4</sup> However, calculations at these lower energies must be done with the curved wave formalism, taking into account the curvature of the outgoing and scattered photoelectron.<sup>5</sup> The tables of Teo and Lee<sup>2</sup> were calculated by using a plane wave approximation for the scattering of the outgoing photoelectron by the neighboring atom. This approximation is unsatisfactory at low photoelectron

momentum especially for higher  $Z$  elements. Curved wave calculations have been performed previously,<sup>3,5</sup> but tabulations have not become available for the general user.

The amplitude and phase shift functions obtained from the curved wave calculations depend on the separation,  $R$ , between the absorbing and the backscattering atoms unlike the case of plane wave calculations, wherein  $R$  is implicitly set of infinity. The dependence on  $R$  is strongest at low  $k$  where the plane wave approximation becomes most unreliable. For physically reasonable variations of interatomic separation, however, the  $R$  dependence is relatively slow. Thus tabulations of  $B(k,R)$  and  $\phi(k,R)$  over the  $k$  range of interest, at two values of  $R$  can adequately serve the general user and obviate the need to recalculate the functions whenever  $R$  is varied. Interpolation may be used to obtain more precise functions at intermediate distances.

We have calculated the amplitude and phase shift functions of nearly every element in the periodic table by using a curved wave formalism. In this paper (in Supplementary Material) we tabulate our results as a function of atomic number at two interatomic separations for approximately half of the elements. Intermediate values of interatomic separation and intermediate values of  $Z$  can be readily interpolated. Results are calculated for  $2 \leq k \leq 20 \text{ \AA}^{-1}$ , thus extending the range of available tabulated functions to both lower and higher  $k$ . With recent improvements in synchrotron sources and instrumentation, EXAFS data are routinely obtained for a wider  $k$  range than Teo and Lee<sup>2</sup> have considered. This paper also provides the first tabulation of amplitude and phase functions for elements heavier than lead. We note that, when the curvature of the photoelectron is considered,

(1) For general references to EXAFS the following review articles are helpful: Stern, E. A. *Contemp. Phys.* 1978, 19, 289. Lee, P. A.; Citrin, P. H.; Eisenberger, P.; Kincaid, B. M. *Rev. Mod. Phys.* 1981, 53, 769. Teo, B. K.; Joy, D. C. *EXAFS Spectroscopy*; Plenum Press: New York, 1981. Hayes, T. M.; Boyce, J. B. *Solid State Phys.* 1981, 37, 173.

(2) Teo, B. K.; Lee, P. A. *J. Am. Chem. Soc.* 1979, 101, 2815.

(3) Müller, J. E.; Schaich, W. L. *Phys. Rev. B* 1983, 27, 6489. See also: Rehr, J. J., et al. *Phys. Rev. B* 1986, 34, 4350. Gurman, S. J.; Binstead, N.; Ross, I. *J. Phys. C* 1984, 17, 143. Barton, J. J.; Shirley, D. A. *Phys. Rev. B* 1985, 32, 1862.

(4) Bunker, G. B.; Stern, E. A. *Phys. Rev. Lett.* 1984, 52, 1990.

(5) Lee, P. A.; Pendry, J. B. *Phys. Rev. B* 1975, 11, 2795. Pettifer, R. F.; McMillan, P. W.; Gurman, S. J. In *Structure of Non-Crystalline Materials*; Gaskell, P. H., Ed.; Taylor and Francis: London, 1977. Pettifer, R. F. In *Trends in Physics 1978*; Woolfson, M. M., Ed.; Hilger: Bristol, 1979. Gurman, S. J.; Pettifer, R. F. *Philos. Mag. B* 1979, 40, 345. Pettifer, R. F. In *X-ray Processes in Solids and Inner-shell Ionizations in Atoms*; Fabian, D. J., Watson, L. M., Kleinpoppen, H., Eds.; Plenum: New York, 1981. Greaves, G. N.; Fontaine, A.; Lagarde, P.; Raouf, D.; Gurman, S. J. *Nature (London)* 1981, 293, 611.

<sup>†</sup> Work supported by the U.S. Department of Energy, Basic Energy Sciences-Materials Science, under contract W-31-109-Eng-38.

<sup>‡</sup> Also at the Department of Physics and Astronomy, Northwestern University, Evanston, IL 60201.

<sup>§</sup> Present address: Department of Physics, Oregon State University, Corvallis, OR 97331.

<sup>⊥</sup> Argonne National Laboratory.

<sup>||</sup> Surface Science Instruments.

the backscattering amplitude and phase shift functions are dependent on the angular momentum of the photoelectron with respect to the absorbing atom. Consequently, the functions differ for K and L edge EXAFS. Both K and L edge EXAFS contain the local atomic structure information. For elements lighter than  $Z \approx 45$ , K edge EXAFS is generally acquired in preference to L edge EXAFS. For those elements, the K edge X-ray energies are more compatible with transmission experiments, the accessible spectral range is more favorable, and overlapping EXAFS from nearby absorption edges is less troublesome. However, for elements heavier than  $Z \approx 45$ , the K edge energies are so high that natural line widths become undesirably broad. Also, very hard X-rays are needed for these measurements. Thus, for  $Z > 45$  L edge EXAFS measurements are generally preferred.

Results for K edges (or more generally, absorption by an s-electron) and for L<sub>III</sub> edges (or more generally, absorption by a p-electron) are tabulated in the Supplementary Material. Care should be taken to ensure use of the proper tabulation.

According to the single scattering theory of EXAFS the modulation of the absorption coefficient,  $\chi(k) \equiv (\mu - \mu_0)/\mu_0$ , can be described with the standard EXAFS equation<sup>1</sup>

$$\chi(k) = (-1)^l \sum_j \frac{B_j(k) N_j}{k R_j^2} \sin [2kR_j + 2\delta_c(k) + \phi_j(k)] e^{-2R_j/\lambda} e^{-2k^2\sigma_j^2} \quad (1)$$

where  $\mu$  is the observed absorption coefficient for the material,  $\mu_0$  is a smooth isolated atom-like absorption,  $B_j$  is the backscattering amplitude from each of the  $N_j$  neighboring atoms in the  $j$ th shell which are located at an average distance  $R_j$  from the absorbing atom. The first exponential accounts for inelastic processes;  $\lambda$  is the electron mean free path for inelastic scattering. The second exponential, containing  $\sigma_j$  (the mean square radial displacement of the atoms about  $R_j$ ), is a Debye-Waller type term. The parameter  $\delta_c(k)$  is the phase shift due to the central atom and  $\phi_j(k)$  is the phase shift due to the backscattering atom. The parameter  $l$  is the quantum number of orbital angular momentum of the outgoing photoelectron with respect to the central atom.

Equation 1 was originally formulated with the plane wave approximation. In this approximation, the backscattering amplitude and phase shift functions are related to the individual partial-wave phase shifts resulting from scattering by the neighboring atoms by

$$B_j(k) e^{i\phi_j(k)} = \frac{1}{k} \sum_{l'} (2l' + 1) (-1)^{l'} e^{i\delta_{l'}} \sin \delta_{l'} \quad (2)$$

With the curved wave formalism (following the notation of Müller and Schaich<sup>3</sup>)  $\chi(k)$  is given by

$$\chi(k) = \sum_j N_j e^{-2R_j/\lambda} e^{-2k^2\sigma_j^2} \text{Im} (e^{2i\delta_0} \sum_{l'} (2l' + 1) e^{i\delta_{l'}} \sin \delta_{l'} H(l, l'; kR_j)) \quad (3)$$

where

$$H(l, l'; kR_j) = \sum_{\bar{l}} (2\bar{l} + 1) \left[ \begin{matrix} l & l' & \bar{l} \\ 0 & 0 & 0 \end{matrix} \right] h_{\bar{l}}^+(kR_j) \quad (4)$$

and

$$\left( \begin{matrix} l & l' & \bar{l} \\ 0 & 0 & 0 \end{matrix} \right)$$

is a  $3j$  symbol, and  $h^+(kR_j)$  is an outgoing Hankel function.<sup>6</sup>

By defining backscattering amplitude and phase shift functions,  $B_j(k, R_j)$  and  $\phi_j(k, R_j)$ , that are functions of the interatomic separation  $R_j$  and the angular momentum,  $l$ , of the core state, eq 3 may be recast into the same form as eq 1. In doing so we retain the form of the traditional EXAFS equation. Thus tabulations of  $B_j(k, R_j)$  and  $\phi_j(k, R_j)$  can be conveniently used with standard EXAFS analysis programs.

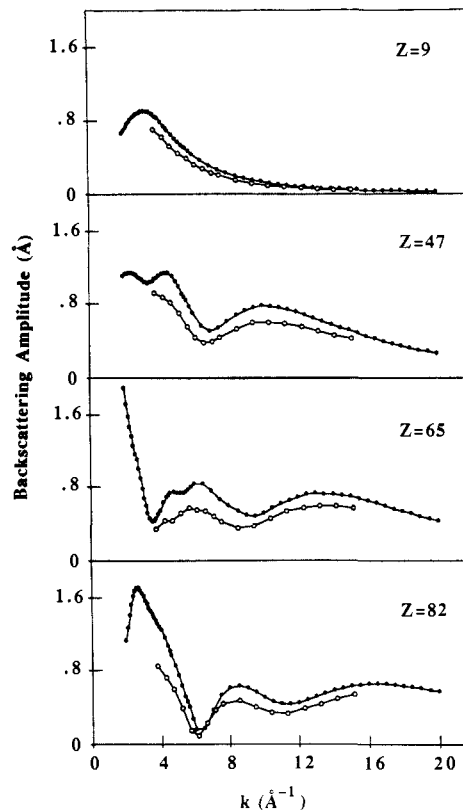


**Figure 1.** Backscattering amplitude function (in Å) versus  $k$  (in Å<sup>-1</sup>) was obtained from plane wave calculations for F ( $Z = 9$ ), Ag ( $Z = 47$ ), Tb ( $Z = 65$ ), and Pb ( $Z = 82$ ) from this work (solid circles) and from Teo and Lee (open circles) [ref 2].

For K-shell absorption (the photoelectron has  $p$  symmetry) the functional relationship is<sup>7</sup>

$$B_j(k, R_j) e^{i\phi_j(k, R_j)} = \frac{kR_j^2}{e^{2ikR_j}} \sum_{l'} (2l' + 1) \times (-1)^{l'} e^{i\delta_{l'}} \sin \delta_{l'} \left( \frac{l' + 1}{2l' + 1} [h_{l'+1}^+(kR_j)]^2 + \frac{l' - 1}{2l' + 1} [h_{l'-1}^+(kR_j)]^2 \right) \quad (5)$$

For L<sub>III</sub>-shell absorption, the photoelectron can have either  $s$  or  $d$  symmetry. However it has been shown that the contribution to  $\chi(k)$  from the  $s$  part is negligible compared to that from the  $d$  part.<sup>2,8</sup> With only the  $d$  contribution<sup>7</sup>

$$B_j(k, R_j) e^{i\phi_j(k, R_j)} = \frac{kR_j^2}{e^{2ikR_j}} \sum_{l'} \left[ (2l' + 1) \times (-1)^{l'} e^{i\delta_{l'}} \sin \delta_{l'} \left\{ \frac{3l'(l' - 1)}{2(2l' + 1)(2l' - 1)} [h_{l'-2}^+(kR_j)]^2 + \frac{l'(l' + 1)}{(2l' + 3)(2l' - 1)} [h_{l'}^+(kR_j)]^2 + \frac{3l'(l' + 2)(l' + 1)}{2(2l' + 3)(2l' + 1)} [h_{l'+2}^+(kR_j)]^2 \right\} \right] \quad (6)$$

The ab initio calculations of EXAFS amplitude and phase functions presented in this work were carried out with the (non-relativistic) Hartree-Fock approximation. The codes used are based on those of Pendry.<sup>9</sup> Modifications were made to meet the requirements of calculating the higher  $l'$  terms required by the curved wave formalism. The Hartree-Fock equation for the

(7) McKale, A. G., et al. *J. Physique, Colloq.* 1986, 47, C8-55.

(8) Heald, S. M.; Stern, E. A. *Phys. Rev. B* 1977, 16, 5549.

(9) Pendry, J. B. *Low Energy Electron Diffraction*; Academic Press: New York, 1974.

(6) For example, see: Messiah, A. *Quantum Mechanics*; North Holland: Amsterdam, 1961; Vol. I.

**Table I.** Backscattering Amplitude (in Å) and Phase Shift (in radians) Functions as a Function of Photoelectron Wave Vector (in Å<sup>-1</sup>) Calculated with the Curved Wave Formalism Appropriate for K Edge Absorption

k	copper (Z = 29)				uranium (z = 92)			
	R = 2.5		R = 4		R = 2.5		R = 4	
	amp	phase	amp	phase	amp	phase	amp	phase
2.0	0.5249	4.9005	0.6975	4.6902	0.5618	10.6931	1.4367	9.0580
2.2	0.3756	4.6973	0.5710	4.4887	0.5426	10.6959	1.2628	8.9681
2.4	0.2706	4.5772	0.4909	4.3099	0.6890	10.6720	1.1329	8.9567
2.6	0.2099	4.6339	0.4466	4.2147	0.8905	10.5058	1.1044	8.9803
2.8	0.1921	4.8550	0.4187	4.2192	1.0833	10.2755	1.1809	8.9994
3.0	0.2052	5.0774	0.3957	4.2943	1.2330	10.0451	1.3048	9.0008
3.2	0.2257	5.2223	0.3735	4.4005	1.3123	9.8162	1.4053	8.9953
3.4	0.2404	5.3221	0.3517	4.5143	1.2972	9.6595	1.4538	8.9511
3.6	0.2521	5.4171	0.3339	4.6322	1.2635	9.5643	1.4860	8.9109
3.8	0.2710	5.5210	0.3267	4.7600	1.2493	9.5311	1.5221	8.8921
4.0	0.3068	5.6179	0.3374	4.8958	1.2678	9.5388	1.5631	8.9033
4.2	0.3678	5.7032	0.3738	5.0326	1.2956	9.5556	1.5901	8.9391
4.4	0.4419	5.7273	0.4284	5.1378	1.2896	9.5607	1.5792	8.9862
4.6	0.5162	5.7234	0.4910	5.2101	1.2217	9.5531	1.5176	9.0336
4.8	0.5813	5.7050	0.5517	5.2564	1.0944	9.5482	1.4111	9.0807
5.0	0.6323	5.6804	0.6037	5.2845	0.9331	9.5741	1.2762	9.1367
5.2	0.6689	5.6544	0.6446	5.2999	0.7731	9.6647	1.1315	9.2150
5.4	0.6950	5.6290	0.6762	5.3061	0.6472	9.8383	0.9919	9.3260
5.6	0.7162	5.6049	0.7023	5.3056	0.5699	10.0691	0.8673	9.4720
5.8	0.7371	5.5816	0.7266	5.3003	0.5259	10.3057	0.7614	9.6487
6.0	0.7598	5.5585	0.7514	5.2919	0.4913	10.5362	0.6748	9.8543
6.5	0.8125	5.4963	0.8087	5.2642	0.4720	11.2347	0.5631	10.5030
7.0	0.8218	5.4252	0.8280	5.2286	0.6160	11.5899	0.6201	11.0241
7.5	0.7919	5.3519	0.8076	5.1813	0.6581	11.6957	0.6899	11.2623
8.0	0.7615	5.2835	0.7802	5.1270	0.6732	11.8478	0.7349	11.4364
8.5	0.7320	5.2117	0.7510	5.0712	0.6651	11.9216	0.7303	11.5605
9.0	0.6794	5.1284	0.7012	5.0071	0.5856	11.9722	0.6753	11.6367
9.5	0.6240	5.0454	0.6468	4.9356	0.5262	12.1260	0.6202	11.7490
10.0	0.5799	4.9662	0.6006	4.8631	0.4781	12.2625	0.5570	11.8854
11.0	0.4847	4.7822	0.5027	4.7042	0.4151	12.6800	0.4580	12.2311
12.0	0.4062	4.6016	0.4206	4.5319	0.4464	12.9894	0.4527	12.6049
13.0	0.3368	4.3979	0.3479	4.3461	0.5369	13.1104	0.5213	12.8157
14.0	0.2851	4.2136	0.2936	4.1641	0.6090	13.1228	0.5881	12.8794
15.0	0.2396	4.0041	0.2460	3.9667	0.6412	13.0552	0.6318	12.8571
16.0	0.2059	3.8266	0.2108	3.7892	0.6667	12.9431	0.6609	12.7790
17.0	0.1761	3.6293	0.1804	3.5971	0.6671	12.8227	0.6645	12.6735
18.0	0.1535	3.4478	0.1561	3.4200	0.6440	12.6793	0.6497	12.5510
19.0	0.1331	3.2726	0.1360	3.2451	0.6237	12.5297	0.6300	12.4169
20.0	0.1177	3.0925	0.1193	3.0694	0.5912	12.3833	0.5993	12.2760

atom plus the external electron is solved by a self-consistent field iterative procedure. The procedure starts from an initial potential constructed from superimposed atomic potentials where the corresponding charge densities are determined from Herman-Skillman-Hartree-Fock-Slater<sup>10</sup> calculations. The atom core is described by the tabulated atomic wave functions and is held frozen during the iterative process. The external electron is allowed to exchange with the atomic wave functions but not to polarize the atom. No elastic effects are taken into account. To obtain the partial wave phase shifts,  $\delta_l$ , the usual procedure was used; the radial Schrodinger equation for an outgoing electron was solved at energy  $E = \hbar^2 k^2 / 2m$  by matching the logarithmic derivative of the radial wave function to that of a free electron at a muffin tin radius. In most cases the muffin tin chosen was 1.5 times the covalent radius. In a few cases (the alkaline earths) a smaller muffin tin was required to obtain proper convergence of the curved wave formulas. The calculation of partial wave phase shifts was terminated when convergence of the backscattering amplitude and phase shift functions was obtained. The backscattering amplitude and phase shift functions for K edge absorption were then calculated by using eq 5. For the tabulations for L<sub>III</sub> edge absorption, eq 6 was used.

The functions in eq 5 and 6 can be calculated relatively easily even on a microcomputer given the individual partial wave phase shifts and the interatomic distances. However the number of partial wave phase shifts for any given calculation is too large for

publication in printed form. As a compromise we use the fact that the functions are weakly dependent on  $R_j$  so that only an approximate interatomic distance need be used for the calculation of  $B_j(k)$  and  $\phi_j(k)$  for a given element. We have tabulated backscattering amplitude and phase shift functions calculated at selected distances for about half of the elements in the periodic table (see Supplementary Material). In Table I and II we provide, as examples of the fuller tables available in the Supplementary Material, the backscattering amplitude and phase shift functions calculated for the two elements, copper and uranium. After Teo and Lee,<sup>2</sup> we use the units of Å for the amplitude function, radians for the phase functions, and Å<sup>-1</sup> for the electron wave vector  $k$ . However, for the  $k$  grid we use a higher point density to get adequate definition of spectral features (Full tabulations of partial wave phase shifts, with a higher point density calculated for nearly every element, with a program to convert them into the backscattering amplitude and phase shift functions will be made available to interested users.).

The type of error that is made by the use of an approximate value of  $R_j$  for calculating  $B_j(k)$  and  $\phi_j(k)$  can be largely compensated for by a small (<1 eV) adjustment of  $E_0$  in fitting eq 1 to experimental data. In eq 1  $k = ((2m/\hbar^2)(E - E_0))^{1/2}$ , where the parameter  $E$  is the photon energy and  $E_0$  is the approximate edge energy so that  $E - E_0$  is the photoelectron kinetic energy. Structural parameters obtained by fitting eq 1 to measured spectra (with  $E_0$ , as usual, being a fit parameter) are quite independent of reasonable variations in  $R_j$  from the crystallographic values.

We have not recalculated the central atom phase shifts  $\delta_c(k)$ . The functions are sufficiently smooth that the tabulations of Teo

(10) Herman, F.; Skillman, S. *Atomic Structure Calculations*; Prentice-Hall: Englewood Cliffs, NJ, 1963.

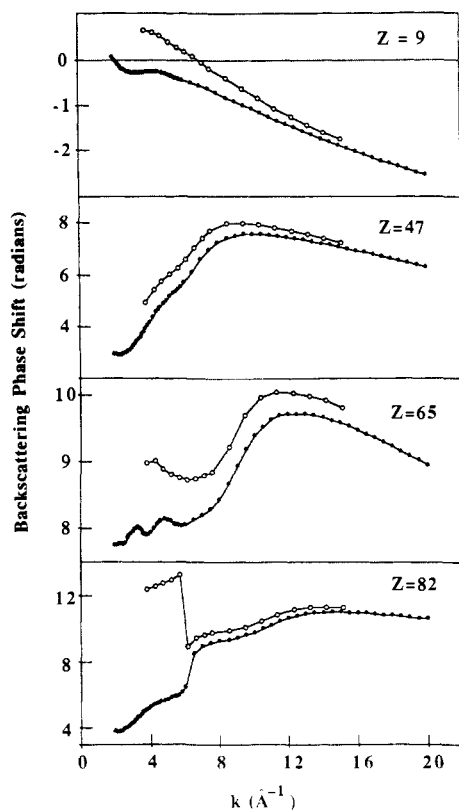


**Figure 2.** Backscattering phase shift function (in radians) was obtained from plane wave calculations versus  $k$  (in  $\text{\AA}^{-1}$ ) for F ( $Z = 9$ ), Ag ( $Z = 47$ ), Tb ( $Z = 65$ ), and Pb ( $Z = 82$ ) from this work (solid circles) and from Teo and Lee (open circles) [ref 2].

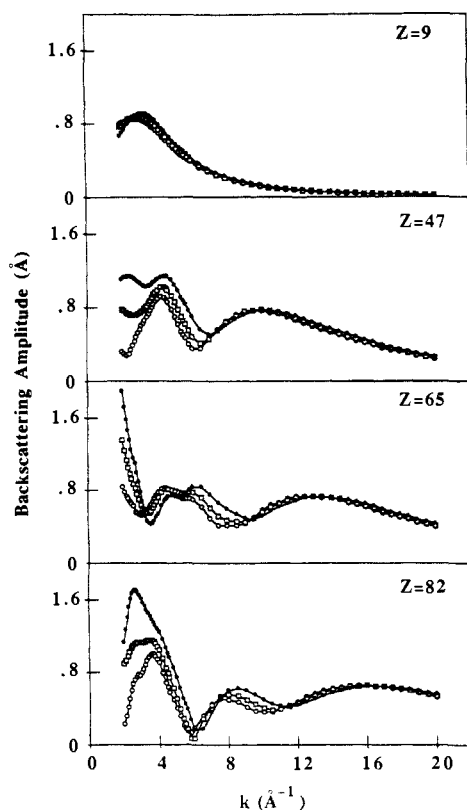


**Figure 3.** Backscattering amplitude function (in  $\text{\AA}$ ) versus  $k$  (in  $\text{\AA}^{-1}$ ) for F ( $Z = 9$ ), Ag ( $Z = 47$ ), Tb ( $Z = 65$ ), and Pb ( $Z = 82$ ) was calculated by using the plane wave approximation at  $R = \infty$  (solid circles), the curved wave formalism at  $R = 4 \text{\AA}$  (open squares), and the curved wave formalism at  $R = 2.5 \text{\AA}$  (open circles).

and Lee<sup>2</sup> can be used with appropriate extrapolation in  $k$ . Like the curved wave amplitude and phase functions,  $\delta_c(k)$  differ for

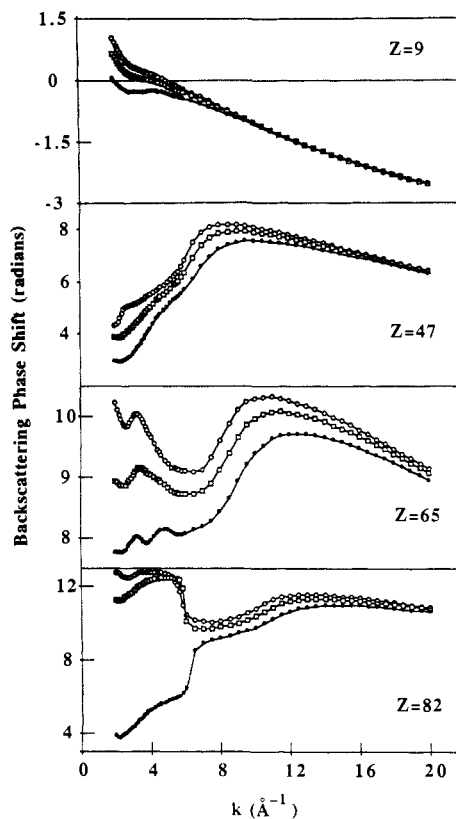


**Figure 4.** Backscattering phase shift function (in radians) versus  $k$  (in  $\text{\AA}^{-1}$ ) for F ( $Z = 9$ ), Ag ( $Z = 47$ ), Tb ( $Z = 65$ ), and Pb ( $Z = 82$ ) was calculated by using the plane wave approximation at  $R = \infty$  (solid circles), the curved wave formalism at  $R = 4 \text{\AA}$  (open squares), and the curved wave formalism at  $R = 2.5 \text{\AA}$  (open circles).

K and  $L_{III}$  edge EXAFS. We caution, however, that the functional form of  $\delta_c(k)$  can be well approximated by the expansion

$$\delta_c(k) = A + Bk + Ck^2 \quad (7)$$

with a large linear term  $B$ . Thus when eq 1 is fit to experimental data, any error in  $B$  will be directly compensated by a corresponding error in  $R_j$ . Consequently, the accuracy of extracted structural parameters obtained from analysis of experimental data is strongly influenced by the central atom phase shift as well as the backscattering functions. Inaccuracies in  $\delta_c$  (resulting, for example, from inadequate treatment of inelastic effects, core hole lifetime effects, and final state screening effects) will directly limit the accuracy of measured structural parameters.<sup>11</sup> EXAFS measurements of carefully selected model compounds can be used with the tabulated backscattering functions to obtain precise adjustments of the coefficient  $B$ . For absorber atoms with  $Z > 82$ , for which  $\delta_c$  has not been calculated, model compounds may also serve to obtain  $\delta_c$ .<sup>12</sup>

In Figures 1 and 2 we show representative backscattering amplitude and phase functions as tabulated by Teo and Lee<sup>2</sup> and those of this study. Both sets of calculations were performed by using the plane wave approximation. For the most part, differences between the results are attributable to differences in the treatment of inelastic effects. The  $k$  dependent structural features in these functions are comparable for the two sets of calculations.

In figures 3 and 4 we show the effect of the curved wave formalism on  $B(k)$  and  $\phi(k)$ . In each figure we show these functions calculated by using a plane wave approximation ( $R = \infty$ ) and by using a curved wave formalism at two different distances ( $R = 4 \text{\AA}$  and  $R = 2.5 \text{\AA}$ ). In general the effects of the curved

(11) Nogura, C.; Spanjaard, D. *J. Phys. F* **1981**, *11*, 1133. Nogura, C.; Spanjaard, D. *J. Phys. F* **1979**, *9*, 1189.

(12) Veal, B. W.; Mundy, J. N.; Lam, D. J. In *Handbook on the Physics and Chemistry of the Actinides*; Freeman, A. J., Lander, G. H., Eds.; Elsevier Science Publishers: 1987.

**Table II.** Backscattering Amplitude (in Å) and Phase Shift (in radians) Functions as a Function of Photoelectron Wave Vector (in Å<sup>-1</sup>) Calculated with the Curved Wave Formalism Appropriate for L Edge Absorption

k	copper (Z = 29)				uranium (Z = 92)			
	R = 2.5		R = 4		R = 2.5		R = 4	
	amp	phase	amp	phase	amp	phase	amp	phase
2.0	0.5713	11.3907	0.6019	5.1545	1.4453	14.3095	0.5321	9.7499
2.2	0.4387	10.7896	0.4789	4.8759	1.6214	14.0563	0.4933	9.5447
2.4	0.3494	10.1941	0.3913	4.6174	1.6457	13.6289	0.4599	9.5800
2.6	0.2849	9.6745	0.3376	4.4458	1.5103	13.1450	0.5038	9.6770
2.8	0.2195	9.2499	0.3031	4.3998	1.2802	12.6363	0.6279	9.6672
3.0	0.1477	8.8559	0.2789	4.4597	1.0064	12.0965	0.7893	9.5755
3.2	0.0858	8.3299	0.2614	4.5760	0.8395	11.2606	0.9487	9.4697
3.4	0.0612	7.4642	0.2483	4.7103	0.7050	10.6156	1.0460	9.3545
3.6	0.0777	6.8379	0.2394	4.8539	0.6094	10.1324	1.1133	9.2621
3.8	0.1090	6.6327	0.2393	5.0122	0.5089	9.8614	1.1696	9.2029
4.0	0.1521	6.5670	0.2553	5.1774	0.4472	9.8428	1.2247	9.1804
4.2	0.2126	6.5548	0.2943	5.3325	0.4787	9.9650	1.2700	9.1867
4.4	0.2898	6.4603	0.3533	5.4358	0.5843	9.9940	1.2869	9.2064
4.6	0.3692	6.3575	0.4205	5.4940	0.6761	9.9079	1.2609	9.2277
4.8	0.4422	6.2579	0.4862	5.5222	0.7012	9.7699	1.1916	9.2495
5.0	0.5027	6.1673	0.5434	5.5321	0.6457	9.6352	1.0894	9.2819
5.2	0.5486	6.0880	0.5897	5.5309	0.5231	9.5506	0.9695	9.3396
5.4	0.5825	6.0209	0.6260	5.5227	0.3706	9.5971	0.8471	9.4351
5.6	0.6094	5.9652	0.6561	5.5100	0.2501	9.9118	0.7344	9.5724
5.8	0.6343	5.9187	0.6837	5.4943	0.2222	10.4426	0.6384	9.7473
6.0	0.6605	5.8780	0.7112	5.4768	0.2469	10.7972	0.5607	9.6564
6.5	0.7264	5.7805	0.7741	5.4295	0.2510	11.4979	0.4661	10.6409
7.0	0.7552	5.6733	0.7999	5.3769	0.4450	11.9659	0.5430	11.1868
7.5	0.7394	5.5697	0.7855	5.3159	0.5341	11.9216	0.6270	11.4068
8.0	0.7164	5.4831	0.7622	5.2515	0.5314	12.0253	0.6785	11.5618
8.5	0.6963	5.3986	0.7364	5.1869	0.5565	12.1039	0.6833	11.6713
9.0	0.6536	5.2992	0.6902	5.1147	0.5035	12.0874	0.6360	11.7341
9.5	0.6033	5.2031	0.6383	5.0366	0.4314	12.2305	0.5840	11.8370
10.0	0.5623	5.1166	0.5937	4.9589	0.4028	12.3895	0.5253	11.9670
11.0	0.4760	4.9168	0.4989	4.7903	0.3406	12.8257	0.4305	12.3121
12.0	0.3998	4.7253	0.4182	4.6110	0.3922	13.1371	0.4303	12.6910
13.0	0.3340	4.5117	0.3467	4.4191	0.4961	13.2584	0.5028	12.8998
14.0	0.2827	4.3204	0.2928	4.2321	0.5706	13.2606	0.5730	12.9574
15.0	0.2386	4.1038	0.2456	4.0306	0.6103	13.1697	0.6197	12.9277
16.0	0.2049	3.9213	0.2105	3.8492	0.6441	13.0499	0.6509	12.8438
17.0	0.1755	3.7173	0.1802	3.6538	0.6456	12.9222	0.6562	12.7337
18.0	0.1532	3.5336	0.1560	3.4739	0.6277	12.7671	0.6431	12.6068
19.0	0.1327	3.3516	0.1359	3.2960	0.6115	12.6142	0.6246	12.4692
20.0	0.1176	3.1702	0.1193	3.1182	0.5794	12.4622	0.5949	12.3254

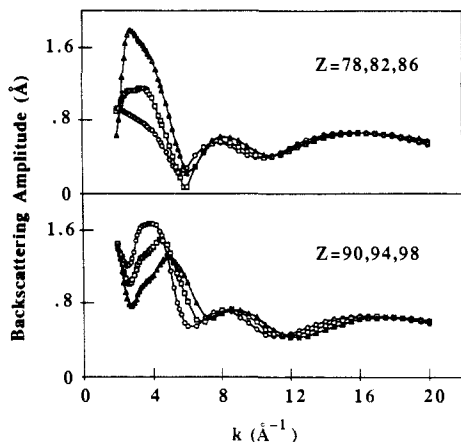


**Figure 5.** Backscattering amplitude function (in Å) versus  $k$  (in Å<sup>-1</sup>) for Pt ( $Z = 78$ , circles), Pb ( $Z = 82$ , squares), Rn ( $Z = 86$ , triangles), Th ( $Z = 90$ , circles), Pu ( $Z = 94$ , squares), and Cf ( $Z = 98$ , triangles) was calculated by using the curved wave formalism at  $R = 4$  Å.

wave formalism are more prominent at low  $k$ . However, for heavy elements the effects are quite pronounced to much higher values of  $k$ . The anomalous behavior of these functions for Pb has been explored in more detail elsewhere.<sup>13</sup>

In Figures 5 and 6 we show the systematic behavior of the amplitude and phase functions for  $Z > 82$ . The systematics of

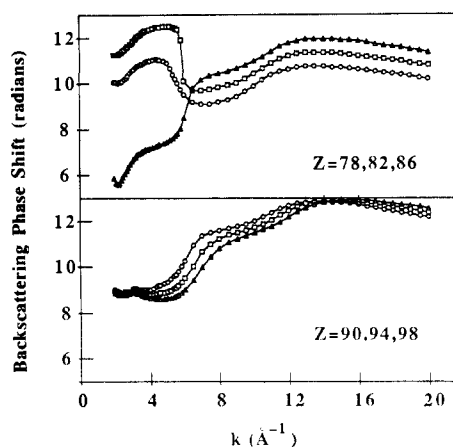


**Figure 6.** Backscattering phase shift function (in radians) versus  $k$  (in Å<sup>-1</sup>) for Pt ( $Z = 78$ , circles), Pb ( $Z = 82$ , squares), Rn ( $Z = 86$ , triangles), Th ( $Z = 90$ , circles), Pu ( $Z = 94$ , squares), and Cf ( $Z = 98$ , triangles) was calculated by using the curved wave formalism at  $R = 4$  Å.

these functions are presented here for the first time. (The tabulations of Teo and Lee<sup>2</sup> stopped at  $Z = 82$ .) As previously observed experimentally,<sup>14</sup> the abrupt phase change (near  $k = 6$  Å<sup>-1</sup>) in these functions for elements with  $Z$  near 82 becomes

(13) McKale, A. G.; et al., submitted to *Phys. Rev. B*.

(14) Knapp, G. S.; McKale, A. G.; Chan, S.-K.; Veal, B. W. In *SPIE Vol. 690—X-rays in Materials Analysis: Novel Applications and Recent Developments*; SPIE: Bellingham, WA, 1986.

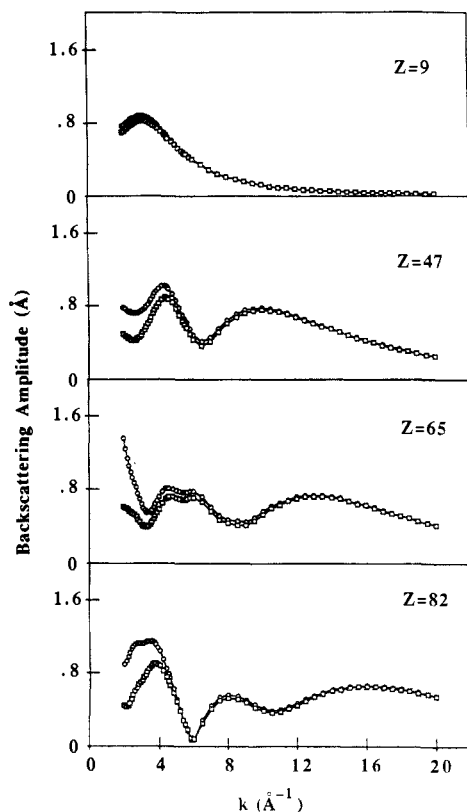


**Figure 7.** Backscattering amplitude function (in Å) versus  $k$  (in  $\text{\AA}^{-1}$ ) was calculated by using the curved wave formalism appropriate for K edge absorption (circles) and appropriate for L edge absorption (squares) for F ( $Z = 9$ ), Ag ( $Z = 47$ ), Tb ( $Z = 65$ ), and Pb ( $Z = 82$ ).

significantly smaller as  $Z$  increases.

In Figures 7 and 8 we compare representative backscattering amplitude and phase functions calculated by using the curved wave formalism appropriate for K edge EXAFS and appropriate for L edge EXAFS with an interatomic separation of 4 Å. The difference between the two calculations is most pronounced at small  $k$ . Indeed the difference between the K and L edge functions (at fixed  $R$ ) is very similar to the difference between two K edge functions with different  $R$  values.

We have tested our calculations on a number of systems with generally favorable results. The use of the curved wave formalism with  $\delta_c(k)$  from Teo and Lee<sup>2</sup> consistently yields better structural parameters than does a plane wave calculation.<sup>7,14,15</sup> Because we have not taken into account any inelastic effects or multi-electron processes, an overall scale factor is required for comparing the theoretical amplitude with experiment. A scaling limitation also pertains to the results of Teo and Lee<sup>2</sup>. Note, however, that a somewhat different scaling is required for the two sets of tables.

The tabulation of the curved wave functions in the same basic format as that of Teo and Lee<sup>2</sup> makes it possible to use them in exactly the same manner as the calculated functions were previously used. However, these functions provide the capability to analyze experimental data much closer to the absorption edge than was previously possible. The ability to analyze low  $k$  data is especially important for the study of disordered systems and materials that contain backscattering atoms of low atomic number. These EXAFS spectra decay rapidly with increasing  $k$  with the

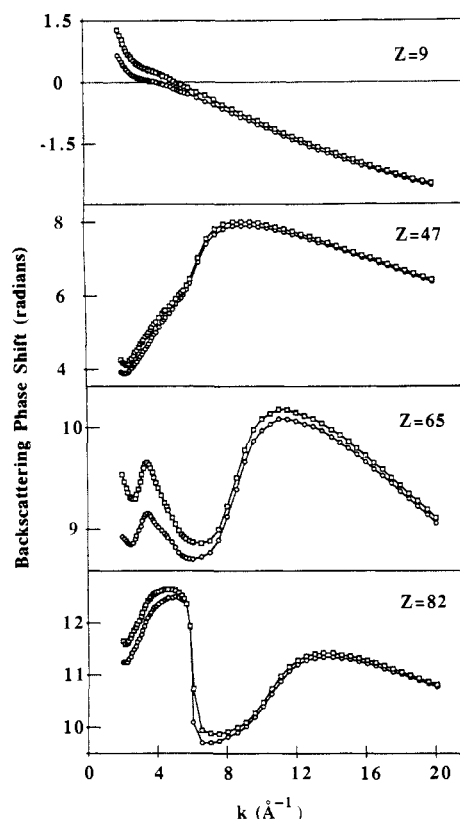


**Figure 8.** Backscattering phase shift function (in radians) was calculated by using the curved wave formalism appropriate for K edge absorption (circles) and appropriate for L edge absorption (squares) for F ( $Z = 9$ ), Ag ( $Z = 47$ ), Tb ( $Z = 65$ ), and Pb ( $Z = 82$ ).

consequence that the usable spectral window is small, and, furthermore, it is confined to low  $k$ .

The  $k$  range of the calculated functions has also been extended to higher  $k$ , and functions have been calculated for those elements with  $Z > 82$ . In general, use of the curved wave formalism should provide improvement in the accuracy of the calculated functions with consequent improvement in the determination of structural parameters from EXAFS data.

**Acknowledgment.** We would like to thank Anne Gershenson for her assistance with computation. Work was supported by the U.S. Department of Energy, Basic Energy Sciences-Materials Science, under contract W-31-109-Eng-38.

**Registry No.** B, 7440-42-8; N, 17778-88-0; F, 14762-94-8; Na, 7440-23-5; Al, 7429-90-5; P, 7723-14-0; Cl, 22537-15-1; K, 7440-09-7; Sc, 7440-20-2; V, 7440-62-2; Mn, 7439-96-5; Co, 7440-48-4; Cu, 7440-50-8; Ga, 7440-55-3; As, 7440-38-2; Br, 10097-32-2; Rb, 7440-17-7; Y, 7440-65-5; Nb, 7440-03-1; Tc, 7440-26-8; Rh, 7440-16-6; Ag, 7440-22-4; In, 7440-74-6; Sb, 7440-36-0; I, 14362-44-8; Cs, 7440-46-2; La, 7439-91-0; Pr, 7440-10-0; Pm, 7440-12-2; Eu, 7440-53-1; Tb, 7440-27-9; Ho, 7440-60-0; Tm, 7440-30-4; Lu, 7439-94-3; Ta, 7440-25-7; Re, 7440-15-5; Ir, 7439-88-5; Au, 7440-57-5; Tl, 7440-28-0; Bi, 7440-69-9; At, 7440-68-8; Fr, 7440-73-5; Ac, 7440-34-8; Th, 7440-29-1; Pa, 7440-13-3; U, 7440-61-1; Np, 7439-99-8; Pu, 7440-07-5; Am, 7440-35-9; Cm, 7440-51-9; Bk, 7440-40-6; Cf, 7440-71-3; Pb, 7439-92-1; Pt, 7440-06-4; Rn, 10043-92-2.

**Supplementary Material Available:** Tables S1 (for K absorption edges) and S2 (for Lu<sub>III</sub> absorption edges) listing the backscattering amplitude and phase functions for approximately half of the elements from boron through californium (53 pages). Ordering information is given on any current masthead page.

(15) McKale, A. G.; Knapp, G. S.; Chan, S.-K. *Phys. Rev. B* **1986**, *33*, 841.